

Effect of running vehicles on airflow field around highway embankment area

Ying Jia¹⁾, Sheng Zhang²⁾, Bing Han³⁾ and * Jie Li⁴⁾

^{1),2),3)}School of Civil Engineering, Beijing Jiaotong University,
No.3 Shang Yuan Cun, Hai Dian District, Beijing 100044, P. R. China
²⁾Department of Fundamental Course, Beijing Institute of Clothing Technology,
NO.2 Yinghua Road Chaoyang District, Beijing 100029, P. R. China
¹⁾yjia@bjtu.edu.cn
⁴⁾jackeyz8@163.com

ABSTRACT

A numerical simulation of atmospheric flow field around a highway embankment area with vehicles in motion is carried out by means of RNG $k-\varepsilon$ turbulence model. The effect of running vehicles with different assembly on the flow field around highway embankment area is analyzed, in the case of different embankment height and different grade of side slope. The calculation results show that, in the operation with running vehicle, flow field around highway embankment shows different changes under different conditions. In addition, the influence of a single vehicle on the flow field is very different from that of motorcades.

1. INTRODUCTION

In recent years, the construction of highway promotes the development of society and coastal economy. However, during the construction and using of the highway, the ecological environment (including atmospheric environment) along the highway is affected inevitably. The construction of highway makes relative stability of airflow field in original areas confused, and furthermore the vehicles running on the highway disturb the flow field around highway areas, making the distribution of flow field more complex, which might convert the diffusion of automobile exhaust, fugitive dust and

1) Professor

2) Graduate Student

3) Professor

4) Professor

other pollution and affect atmospheric environment along the highway.

Zhou *et al.* (2007) simulated a large range of complex terrain region (23km × 27km) flow in complex terrain, and compared the results of wind tunnel test with the numerical simulation, which provides a reference for the simulation of similar large-scale regional flow field. In addition, Maruyama *et al.* (2006) has pointed out that there was the obvious wind-gathering characteristics for some special structures like highway long-span bridge; Sigbjörnsson and Snæbjörnsson (1988) found out that some topographic features could lead to the amplified areas of local wind where many traffic accidents occurred; Maurizi *et al.* (1988) simulated the local flow field of 1000m-height mountain by adopting non orthogonal grid systems and obtained the distribution of flow velocity in those areas 30m above the ground; Uchida and Ohya (2003) simulated the flow field of a 9.5km×5km mountain terrain by the large eddy simulation method.

Besides the simulation of flow field, the simulation of relative motion simulation is often used in some publications. Sun *et al.* (2011) carried out numerical simulation of the external flow field with two vehicles during the overtaking process by adopting the dynamic mesh and sliding interface technique, indicating the transient variety trend of drag and side force of vehicles; the transient aerodynamic characteristics of vehicles during the overtaking process was also analyzed by intercepting the flow profile of the pressure field and velocity field. Fu *et al.* (2007) numerically simulated the aerodynamic characteristics of external flow field during the vehicles overtaking process, respectively in the steady-state and in the transient state.

However, most of the current researches on flow field simulation mainly concentrate on the bridge, the wind resistance performance of building, or the effect of train running performance, and there is a little research on flow field of highway region with vehicles driving. Therefore, it is necessary and significant to study the effect of traveling vehicles on flow field in highway area.

2. THEORETICAL ANALYSIS AND NUMERICAL SIMULATION

In order to study the effect of running vehicle on flow field, both the flow field and the relative motion of flow are simulated numerically in this paper. On the basis of the principle theory of computational fluid dynamics, the model of RNG k- ϵ turbulence (Yakhot and Orzag 1996) and the method of finite volume and sliding mesh technique are adopted.

2.1 Basic governing equations

When vehicles are traveling on the highway, the flow field of highway area is in viscous, unsteady and incompressible flow state with typical three-dimensional separating flow characteristics, which follows three conservation equations on mass, momentum and energy (Wang 2004). The general conservation form of the three

equations is as follows:

$$\frac{\partial(\rho\phi)}{\partial t} + \operatorname{div}(\rho\bar{u}\phi) = \operatorname{div}(\Gamma \operatorname{grad}\phi) + S \quad (1)$$

where: \bar{u} is the velocity vector; t is time; ϕ is global variables; Γ is the generalized diffusion coefficient; S is the term of generalized source. There are specific expressions for ϕ , Γ and S .

2.2 Parameters in computational model

Herein, a four-lane highway model with design speed of 100km/h and the MIRA standard order-back (Le Good and Garry 2004) car model are adopted. The heights of the embankment are $H = 2m$, $4m$ and $5m$ and the slope gradients are $1:1$ and $1:2$. Also, the speed of the vehicles is $90km/h$ and the longitudinal spacing between adjacent vehicles is $50m$.

2.3 Computational domain and meshing

The size of computational domain is $500 m \times 500 m \times (100+2H) m$, as shown in Fig. 1. The origin of coordinate system is located at the bottom center of the highway, and the x -axis is the direction along which the flow comes from, the y -axis is the longitudinal direction along the highway embankment, and the z -axis is the direction vertical to the surface of embankment.

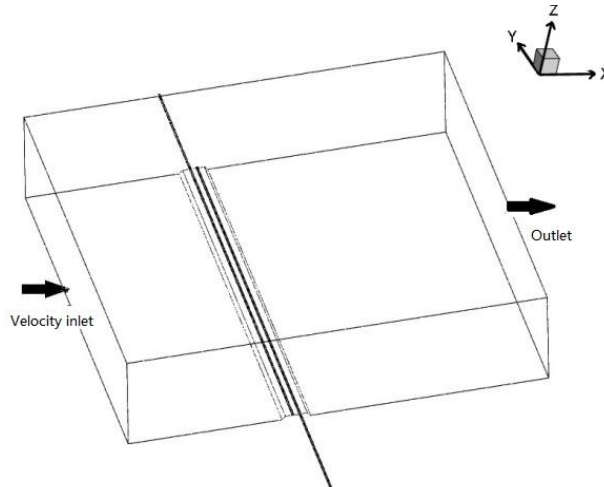


Fig. 1 Computational domain and coordinate system

The size function is used to control quantity and quality of the meshes. Due to the complex shape of the vehicle, each vehicle is meshed separately by means of partition meshing with small initial mesh size and growth rate.

2.4 Boundary conditions

The stream velocity is taken as the inlet boundary condition, and the inlet velocity is about 20m/s, utilizing average wind profile with exponential rate. The boundary condition of the entrance turbulence intensity is described by turbulent kinetic energy

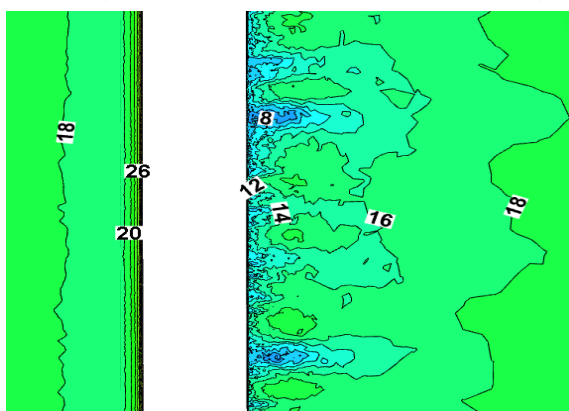
$$k(z) = 1.5[I(z)\bar{u}(z)]^2 \text{ and the turbulent dissipation rate } \varepsilon(z) = \frac{C_{\mu}^{0.75}k(z)^{1.5}}{l}.$$

The top wall and side walls of the computational domain are walls of free slip; a fully developed flow boundary condition is used in the outflow; the pavement, slope walls and the ground are no-slip walls; and the moving walls are used for the vehicle surfaces.

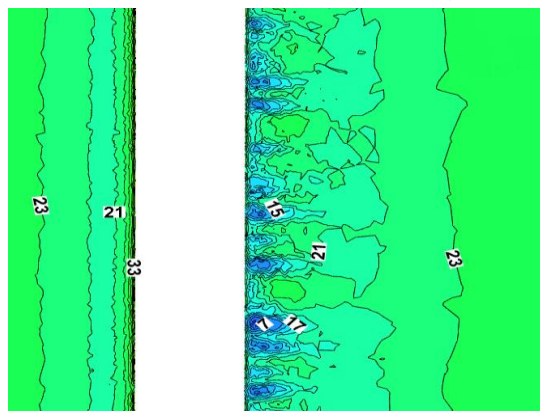
3. ANALYSIS OF NUMERICAL RESULTS

3.1 Effect of a single running vehicle on flow field

Figures 2(a)-(b) shows the flow field distribution of highway embankment area when the embankment height H is 6m and the slope gradient is 1:1, with no traveling vehicle and a single traveling vehicle. The speed of the single vehicle is 90km/h.



(a) No vehicle traveling



(b) A single vehicle traveling

Fig. 2 Contour maps of flow velocity in the horizontal plane of $z=6.0\text{m}$

Figures 2(a)-(b) shows that: (1) the flow velocity on the leading edge of highway embankment is 33m/s and 26m/s, respectively for a single vehicle traveling and for no vehicle traveling; (2) in the back area of highway embankment, the velocity contours is intensive and the gradient of velocity is significant with a single vehicle traveling; when there is no vehicle traveling, the gradient of velocity is relatively smaller; (3) due to the impedance of the highway, the flow velocity in the back of embankment decreases and the vortex forms; with the increasing of distance from observation point to embankment, the variety of flow field levels off gradually, and correspondingly the vortex weakens.

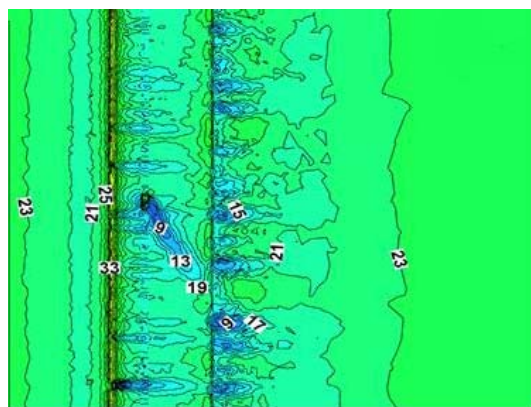


Fig. 3 Contour of flow velocity in horizontal plane of $z=6.1\text{m}$ with a single vehicle traveling

Figure 3 illustrates the contour map of horizontal flow velocity with a single vehicle traveling in the horizontal plane of $z = 6.1\text{m}$, which is a sectional plane across the vehicle body. It can be seen from Fig.3 that when a single vehicle is running, a portion of airflow bypasses the vehicle, and the velocity is reduced and the direction is changed, with vortex produced behind the vehicle. When the direction of the flow stream is perpendicular to the driving direction, an affected area of flow field is formed behind the vehicle, with a rate of flow velocity varying from 9m/s to 19m/s, and the influence scope of a single vehicle on the back areas of vehicle is about 25m.

Figures 4-5 are contour maps of flow velocity in cross-sections (crossing the vehicle body) of $y=-23\text{m}$.

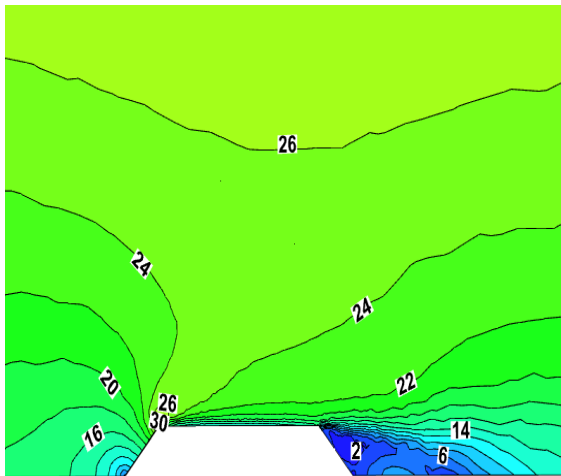


Fig.4 Contour of flow velocity with no vehicle running ($y=-23m$)

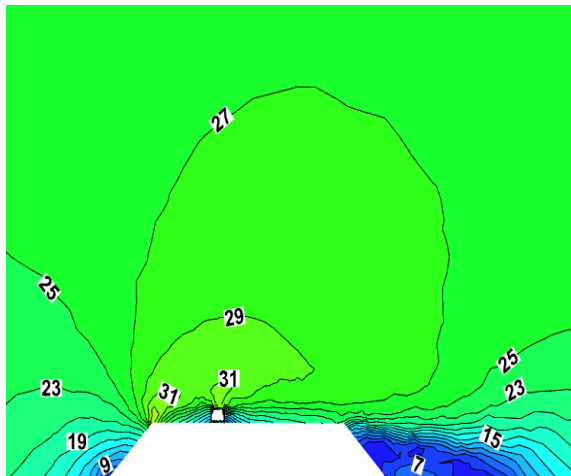


Fig.5 Contour of flow velocity with a single vehicle running ($y=-23m$)

It can be seen from Figs. 4-5 that, in the front side of the embankment where the stream flowing goes forward, the flow velocities in both conditions change suddenly and reach the maximum. When there are no vehicles running, the maximum velocity at the leading edge of the embankment is about 30m/s, and the airflow in other areas changes gently; when there is a single vehicle running, the maximum flow velocity at the leading edge of the embankment is about 33m/s, while in other areas, the distribution of the flow field along the height of the embankment changes due to the impact of running vehicle, which is significantly different from that under no vehicle traveling.

3.2 Effect of running vehicle on flow field in different height of embankment

The slope gradient of embankment is set as 1:1. The inflow velocity is 20m/s, and the driving speed of a single vehicle is 90km/h, with embankment height of 2m, 4m, 6m, and 8m, respectively.

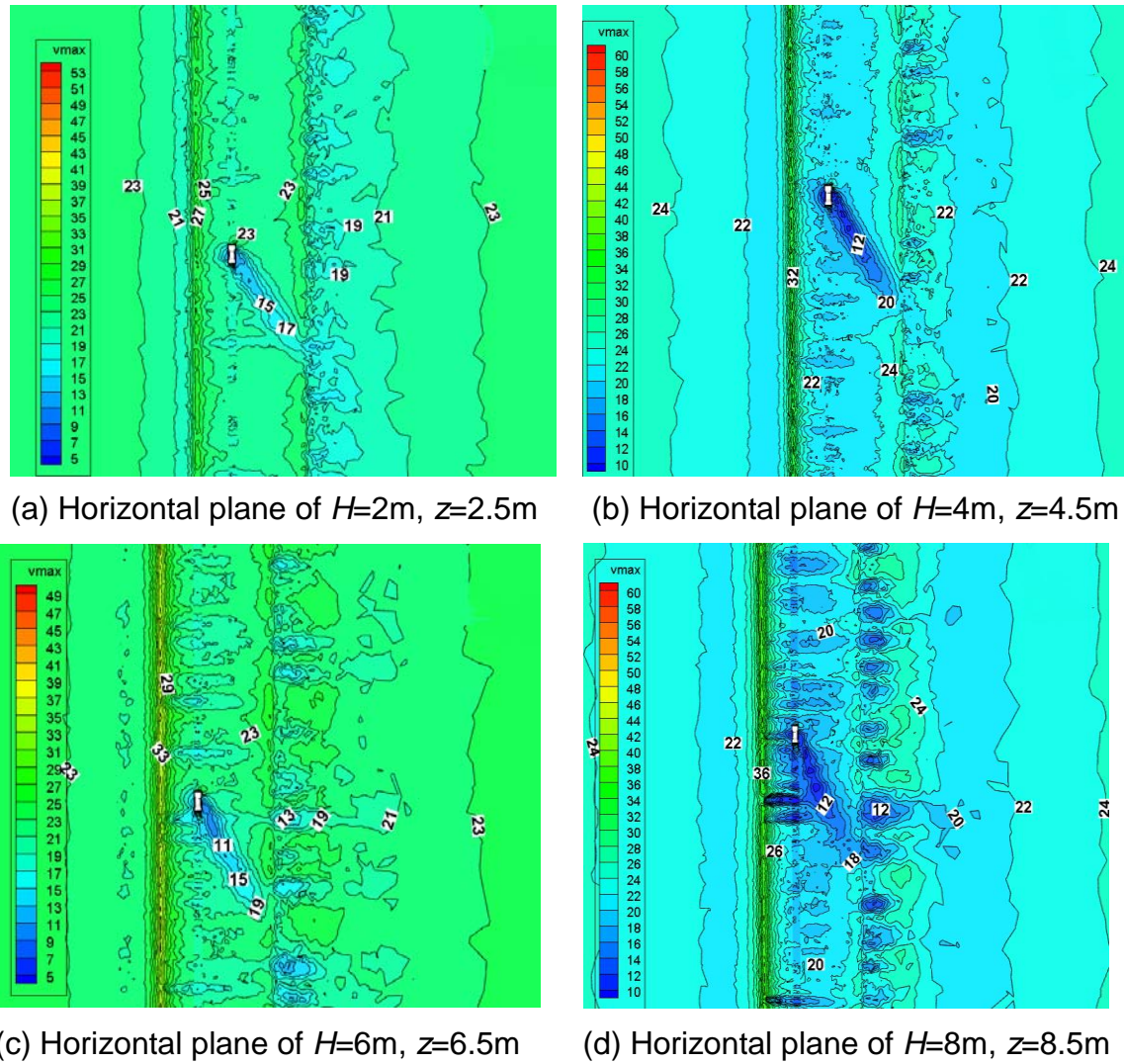


Fig. 6 Contours of flow velocities in a horizontal plane with different embankment height

When there is a single running vehicle, it can be seen from contour map of flow field in Figs. 6(a)-(d) that: with the increasing of the embankment height, the maximum velocity of the flow field at the leading edge of the embankment increases, and the vortex in the leeward side of the embankment enhances. The reason is that the impedance of embankment height to the flow increases due to the increasing of height, which thus makes the flow velocity in the leeward side reduce.

The distribution of the flow field in Figs. 6(a)-(d) shows that an obviously affected area of weak flow forms behind the single running vehicle, whose velocity distribution is different from those in other regions. The velocity is small where it is close to vehicle, and it increases with the distance to vehicle getting larger. The range of influenced areas along the longitudinal direction of the embankment is shown in Fig. 6(a)-(d). When the height of the embankment H is 2m, 4m or 6m, the influence of the wake flow

on the flow field 25m outside the vehicle rear becomes weak; while it is about 35m when the height of the embankment H is 8m. This is because the flow velocity at the leading edge of the embankment increases with the embankment height and the coupling of the flow velocity and the flow brought by the running vehicle becomes strong, and thus the affected area behind the vehicle gets larger.

3.3 Effect of a single running vehicle on flow field with different embankment slopes

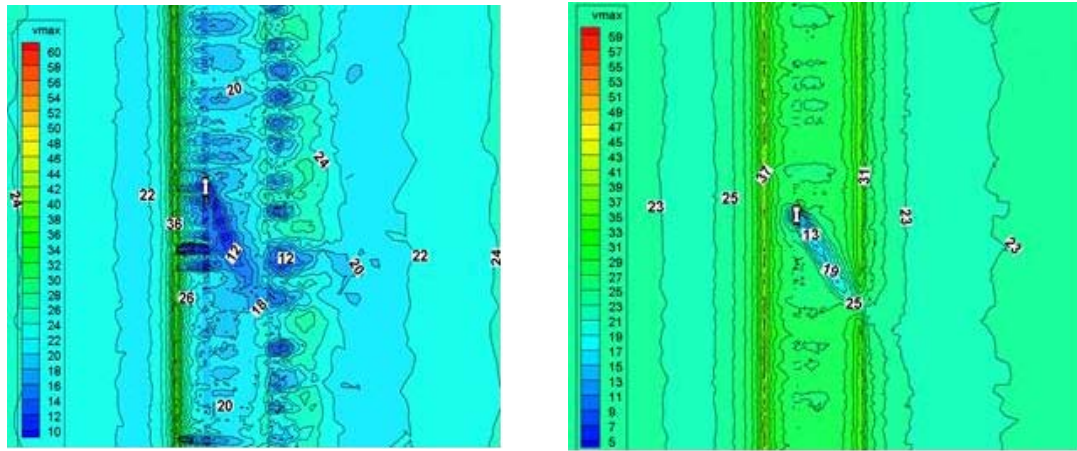
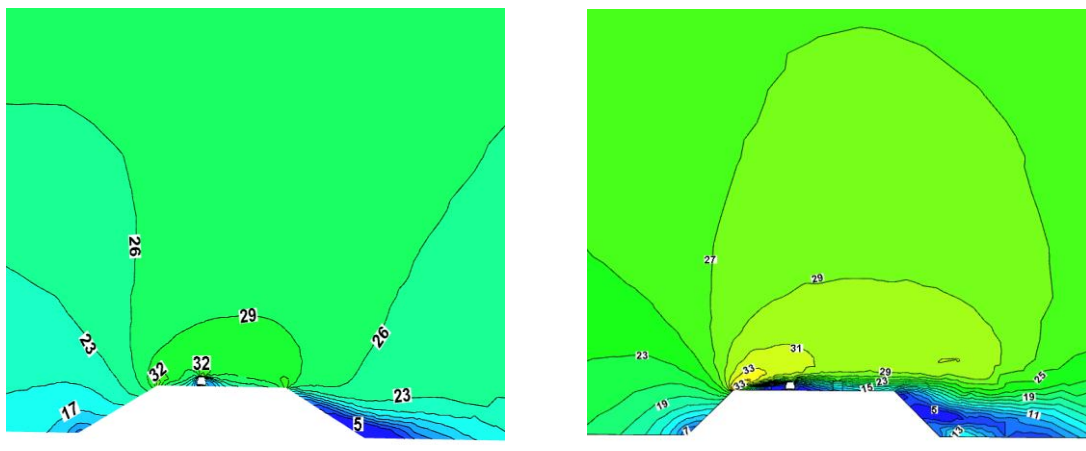


Fig. 7 Contours of flow velocities in a horizontal plane with different slope gradients

Figures 7(a)-(b) illustrates the contour maps of flow velocities in flow field in the cases of embankment height of $z=8\text{m}$ and $z=8.5\text{m}$ and slope gradient of 1:1 and 1:2. It can be seen that: (1) the flow velocity in the slope of 1:1 is smaller than that in the slope of 1:2; (2) the affected area of wake flow is produced by traveling vehicle in both conditions. When the slope gradient is 1:1, the scope of the affected area is 35m along the longitudinal direction of the embankment; and when the slope gradient is 1:2, it is 25m.

Figures 8(a)-(b) contain the contour maps of flow velocity of a sectional plane where $y=2\text{m}$ in different slope gradients, with the embankment height H of 8m. Figures 8(a)-(b) indicates that in the direction of the embankment height, the distribution area of high velocity in the slope gradient of 1:1 is greater than that in the slope gradient of 1:2.

Thus, it is clear that for the highway with 8m embankment height, a 1:2 slope gradient can narrow the affected area of wake flow of the vehicle and can improve the traffic environment.



(a) Slope gradient: 1:2

(b) Slope gradient: 1:1

Fig. 8 Contours of flow velocity in the sectional plane of $y=2m$

3.4 Effect of different running motorcade modes on flow field

The embankment height is assumed to be 8m, and the slope gradient is 1:1. The net distance between vehicles along driving direction of the same motorcade is 50m, and that spacing between vehicles in two-lane is 25m. The form of motorcade traveling is divided into three cases:

- (1) Two motorcades traveling in same direction (Fig. 9);
- (2) Two motorcades traveling in opposite directions (Fig. 10);
- (3) Vehicles travelling in four lanes, two motorcades each direction (Fig. 11).

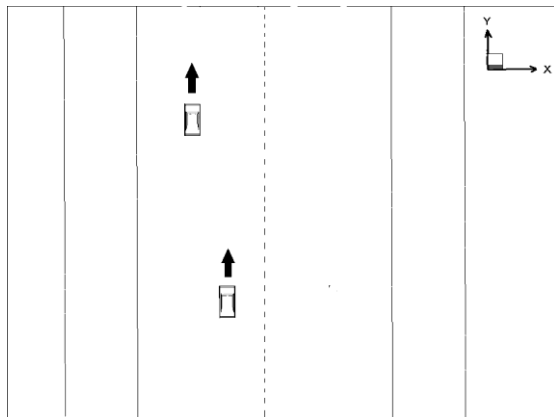


Fig. 9 Two motorcades running
in same direction

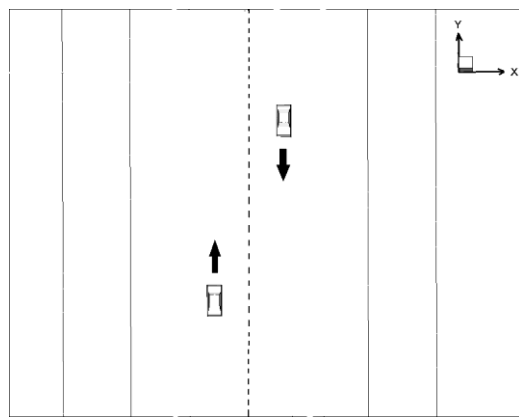


Fig. 10 Two motorcades running
in opposite direction

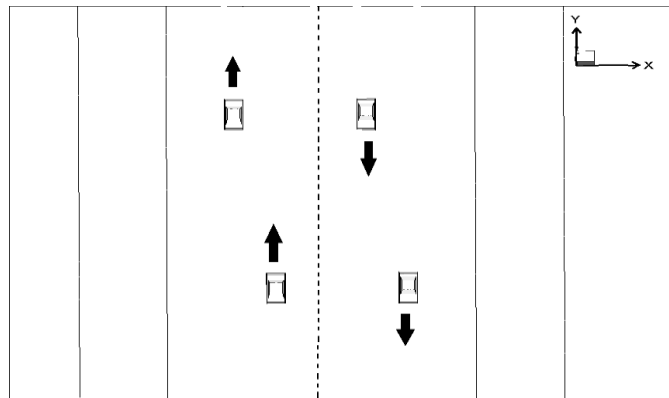


Fig. 11 Vehicles running in all four lanes

3.4.1 Effect of two running motorcades in same direction on the flow field

Figure 12 shows the flow velocity contour map of the flow field in the horizontal plane of $z=8.5\text{m}$ when two motorcades are traveling in the same direction, and Fig. 13 is the map of flow velocity vector. The net lateral spacing between two motorcades is 2.2m, and due to that narrow lateral spacing, the disturbed airflow behind the vehicle in the left lane and the airflow in front of the vehicle in the right lane are coupled. It can be seen from Figs. 12-13 that motorcades in same traveling direction have a greater impact on the flow field and a larger scope of influence than a single traveling vehicle. The maximum velocity at the leading edge of the embankment is about 35m/s.

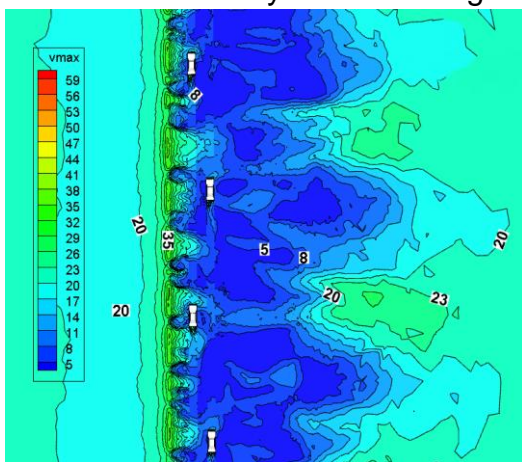


Fig. 12 Flow velocity contour map of the flow field in the horizontal plane of $z=8.5\text{m}$

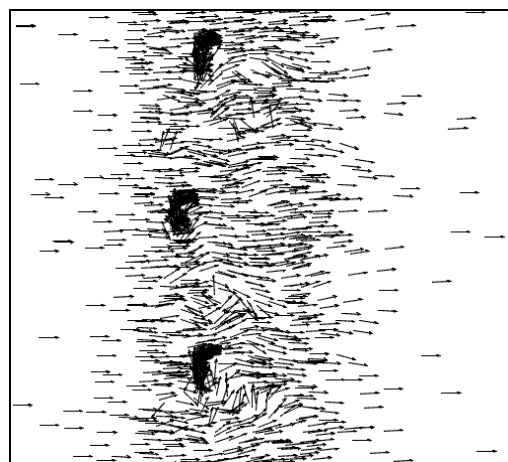


Fig. 13 Vector map of local flow velocity in the horizontal plane of $z=8.5\text{m}$

3.4.2 Effect of two running motorcades in opposite directions on the flow field

The net lateral spacing between two motorcades is 6.7m when two motorcades travel in opposite directions. Fig. 14 is the flow velocity contour map of the flow field in the horizontal plane of $z=8.5\text{m}$, and Fig. 15 is the vector map of flow velocity.

As is shown in Figs. 14-15, the net lateral spacing between vehicles traveling in the

opposite direction is larger than that spacing between vehicles traveling in same direction, so the coupling of airflow between the two motorcades is weaker. The maximum flow velocity at the leading edge of the embankment is about 35m/s, which is close to that with motorcades traveling in the same direction. The distribution of flow field in the leeward side of the embankment shows greater variety.

It can be followed that when two motorcades travel in different directions, their effects on the flow field at the leading edge of the embankment is similar, while that effect in the leeward side is different.

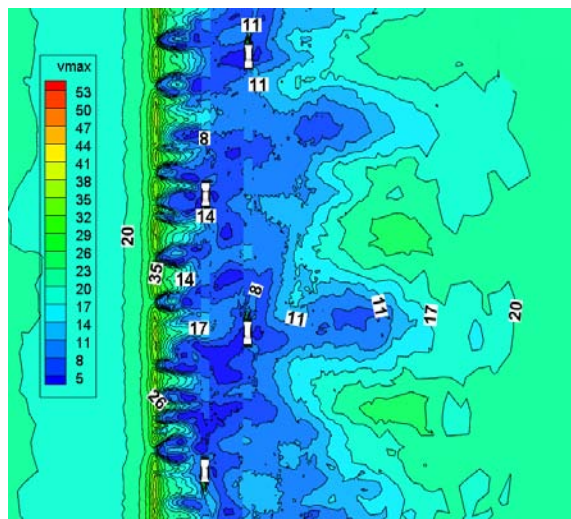


Fig.14 Contour of flow velocity in the horizontal plane of $z=8.5\text{m}$

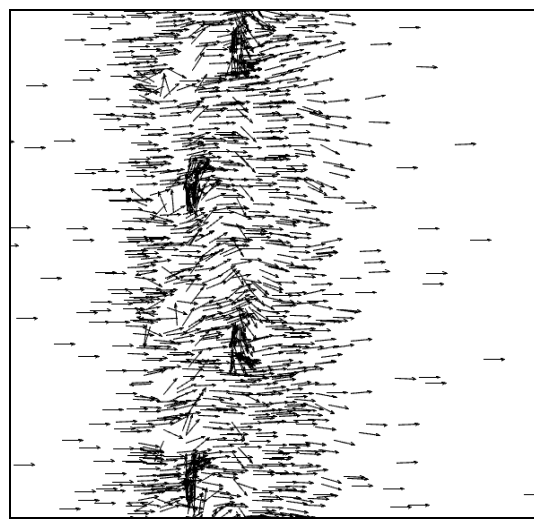


Fig.15 Vector map of local flow velocity in the horizontal plane of $z=8.5\text{m}$

3.4.3 Effect of four lanes vehicles running on the flow field

Figure 16 shows the contour map of flow velocity in the horizontal plane of $z=8.5\text{m}$ with vehicles traveling on all lanes, and Fig. 17 is the vector map of the flow velocity. It can be seen from Fig. 16 that the maximum velocity at the leading edge of the embankment is about 32m/s, and it is smaller than the maximum velocity in the case of two motorcades traveling. In addition, the great relative changes of the flow distribution in the leeward side of the embankment occur.

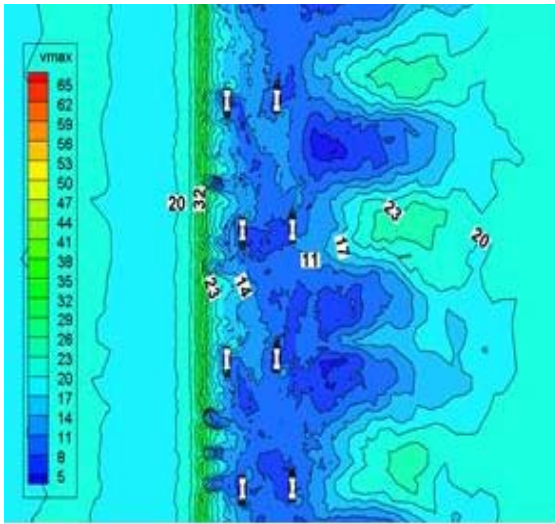


Fig. 16 Contour of flow velocity in the horizontal plane of $z=8.5\text{m}$

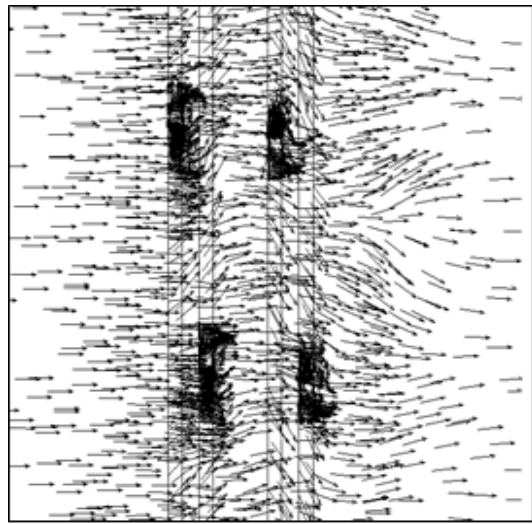


Fig. 17 Vector map of flow velocity in the horizontal plane of $z=8.5\text{m}$

According to the calculated results it can be known that when the motorcades travel in different ways, the mutative law and range of the flow field is similar; the maximum velocity appears in the leading edge of the embankment; due to the coupling of airflow and the traveling vehicle in the pavement area, the variation gradient of the flow velocity changes a great deal. The effect of vehicles traveling on leeward side is greater and the obvious vortex is caused. In the vortex region of flow field, the flow velocity is small relatively, making retention of automobile exhaust, dust and other pollution there, which aggravates the pollutant concentration in the embankment back area. Therefore, the effect of running motorcades on flow field of highway area should be paid more attention.

4. CONCLUSIONS

In this paper, the influence of traveling vehicles on flow field of highway area is studied by means of the theoretical analysis and numerical simulations. From the calculated results, it can be found that some values and phenomenon in the same cross-section are obviously different in the two cases (one with a running vehicle and the other not). Other studies show that different heights and slopes not only affect the velocity of the flow around the embankment and the vehicle, but also make the size of low velocity zone behind the embankment and the distribution area different. What is more, it is clear that when two motorcades travel in different directions, their effects on the flow field at the leading edge of the embankment is similar, while that effect in the leeward side is different. The maximum velocity of four lanes vehicle running reduces by comparing with the case of two motorcades traveling, and the great relative

changes of the flow distribution in the leeward side of the embankment occur. This paper just discusses the effect of running vehicle on flow field of highway embankment regions. However, there are many sections of bridges along highway, which is the next research the authors will carry out in the future.

ACKNOWLEDGMENT

The research is supported by the Projects from National Natural Science Foundation of China (51178033).

REFERENCE

- Maruyama, Y. (2006), "Driving simulator experiment on the moving stability of an automobile under strong crosswind", *J. Wind Eng Ind Aerod.*, **94**(4), 191-205.
- Sigbjörnsson, R. and Snaebjörnsson. J. T. (1988). "Probabilistic assessment of wind related accidents of road vehicles A reliability approach", *J. Wind Eng Ind Aerod.*, 74-76, 1079-1090.
- Maurizi, A., Palma, J.M.L.M., and Castro, F. A. (1988), "Numerical simulation of the atmospheric flow in a mountainous region of the North of Portugal", *J. Wind Eng Ind Aerod.*, **74**, 219-228.
- Uchida, T., and Ohya, Y. (2003), "Large-eddy simulation of turbulent airflow over complex terrain", *J. Wind Eng Ind Aerod.*, **91**(1), 219-299.
- Sun, L., Gu, Z.Q., Yang, Y., Yang, B.H., and Gong, X. (2011), "Analysis of transient aerodynamic characteristics of overtaking and overtaken vehicles", *Journal of Central South University: Science and Technology*, **42**(9), 2681-2686.
- Fu, L.M., He, B.Q., Wu, Y.Z., Hu X. J., and Zhang, Y.C. (2007), "Research on aerodynamic characteristics during the vehicle overtaking process", *Acta Aerodynamica Sinica*, **25**(3), 351-356.
- Yakhot, V., and Orszag, S.A. (1986), *Renormalization group analysis of turbulence. I. Basic theory*. J. Sci Comput, **1**(1), 3-51.
- Le Good, G. M. and Garry, K. P. (2004), "On the use of reference models in automotive aerodynamics", *SAE Technical Paper*, 01-1308.
- Wang F.J. (2004), *Analysis of Computational Fluid Dynamic*, Tsinghua University Press, Beijing, China.
- Zhou, Z.Y., Zhou, Q. and Jiang, B.S. (2007), "Numerical simulation study of wind environment for the flow around large region with complex terrain", *Fourteenth National Conference of Wind Engineering*, Beijing, China, August.